# CHAPTER III

# THEORY

## 3.1 Molecular Sieves for Use in Catalysis

The history of new class of inorganic materials, zeolites and molecular sieves, has been reviewed from the finding of the first zeolite mineral in 1756 through the explosion in new molecular sieve structures and compositions in the 1980's [45]. Zeolites and molecular sieves are finding appliciable acid activity with shape-selectivity features not available in the compositional equivalent amorphous catalysts. In addition, these materials can act as supports for numerous catalytically active metals. Major advances have occurred in the synthesis of molecular sieve materials since the initial discovery of the synthesis zeolite molecular sieve's type A, X and Y, and a great number of techniques have evolved for identifying and characterizing these materials [45]. Added to extensive and ever growing list of aluminosilicate zeolites are molecular sieves containing other elemental compositions. These materials differ in their catalytic activity relative to the aluminosilicate zeolites and may have potential in being customized or tailored for specific applications. Elemental isoelectronic with $Al^{+3}$ or $Si^{+4}$ have been proposed to be substituted into the framework lattice during synthesis. These included $B^{+3}$, $Ga^{+3}$, $Fe^{+3}$, and $Cr^{+3}$ substituting for $Al^{+3}$, and $Ge^{+4}$ and $Ti^{+4}$ for $Si^{+4}$. The incorporation of transition elements such as $Fe^{+3}$ for framework $Al^{+3}$ positions modifies the acid activity and, in addition, provides a novel means of obtaining high dispersions of these metals within the constrained pores of industrially interesting catalyst materials.

## 3.2 Classification of Molecular Sieves

With the recent discoveries of molecular sieve materials containing other elements in addition to, or in lieu of, silicon and aluminium, the casual interchange of the terms "molecular sieve" and "Zeolite" must be reconsidered. In 1932 McBain [45] Proposed the term "molecular sieve" to describe a class of material that exhibited selective adsorption properties. He proposed that for a material to be molecular sieve, it must separate components of a mixture on the basis of molecular size and shape

differences. Two classes of molecular sieves were known when McBain put forth his definition: the zeolites and certain micro porous charcoal. The list now includes the silicates, the metallosilicates, metalloaluminates, the $AlPO_4$'s, and silico- and metalloaluminophosphates, as well as the zeolites. The different classes of molecular sieve materials are listed in figure 3.1 [46]. All are molecular sieves, as their regular framework structures will separate components of a mixture on the basis of size and shape. The difference lies not within the structure of these materials, as many are molecular sieves though none but the aluminosilicates should carry the classical name, zeolite [46].

### 3.2.1 Zeolites

Zeolites are crystalline aluminosilicate that are constructed from $TO_4$ tetrahedral (T= Tetrahedral atom, e.g. , Si, Al) ; each apical oxygen atom is shared with an adjacent tetrahedran [47]. Thus, the ratio of O/T is always equal to 2. A $SiO_4$ unit in framework (structure) is neutral since an oxygen bridges two T atoms and shares electron density with each other (Figure 3.2). However, since Al is +3, for every aluminum containing tetrahedron there is a net -1 charge which must be balanced by cation. The tetrahedra are coordinated such the zeolites have open framework structure with high surface areas. The framework thus obtained contains pores, channels, and cages, or interconnected voids. Access to the cavity is possible through voids of various properties, zeolites are able to be shape and size selective in catalytic molecular rearrangement [45].

Zeolite may be represented by the general formula,

$$M_{x/n}[(AlO_2)_x(SiO_2)_y]_wH_2O$$

where the term in brackets is the crystallographic unit cell. The metal cation of valence n is present to produce electrical neutrality since for each aluminum tetrahedron in the lattice there is an overall charge of -1 [48]. M is a proton, the zeolite becomes a strong Brønsted acid, w is the number of water molecules per unit cell, and x, y are the total number of tetrahedra per unit cell [45].

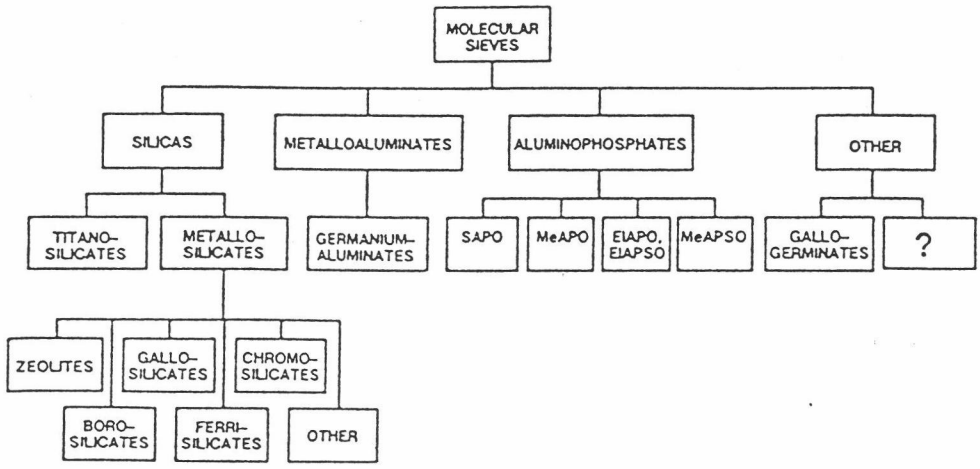


Figure 3.1 Classification of molecular sieve materials indicating extensive variation in composition. The zeolite occupy a subcategory of the metallosilicates [46].

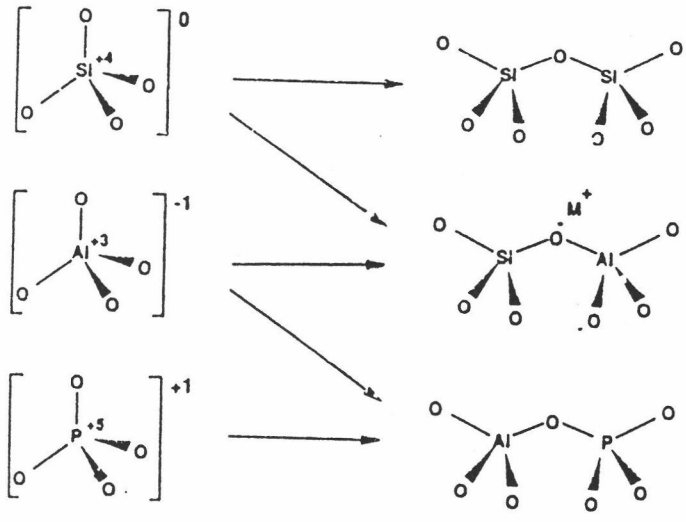


Figure 3.2 Basic building blocks of zeolites-molecular sieves [47].

Approximately 70 distinct structures of zeolites and molecular sieves are known [49]. There are natural zeolites, synthetic analogues of natural zeolites, and synthetic zeolite with no natural counterparts. Their pore sizes range from 4 A° to 13 A°. Zeolites with pores that are comprised of eight T atoms (and eight oxygen atoms) are considered small pore zeolites. They have free diameters of 3.0-4.5 A° , e.g., zeolite A. Medium pore zeolites have pores formed by ten T-atom rings with 4.5-6.0 A° free diameters of 8.0 A° or more, e.g., zeolites X and Y [50]. To date, no zeolite (aluminosilicate) exists with pores larger than ~ 8 A° [47].

In type A zeolite, range cavities are connected through apertures of 0.5 nm, determined by eight-membered rings (Figure 3.3a). The mordenite pore structure consists of elliptical and noninterconnected channels parallel to the c-axis of ortherhombic structure. Their openings are limited by twelve-membered rings (0.6-0.7 nm) (Figure 3.3c) [48].

In silicate and ZSM-5, the tetrahedra are linked to form the chain-type building block [46]. The chains can be connected to form a layer, as shown in Figure 3.4 [51]. Ring consisting of five O atoms are evident in this structure; the name pentasil is therefore used to describe it. Also evident in Figure 3.4 are rings consisting of 10 oxygen atoms; neighboring layers being related either by the operation of a mirror or an inversion. The former pertains to the zeolite ZSM-11, the latter to silicalite or ZSM-5; the intermediate structures constitute the pentasil series.

The three-dimensional structure of silicate (and ZSM-5) is represented in Figure 3.5 a [51]. The ten-membered rings (ca. 0.55 nm in diameter) (Figure 3.3b) provide access to a network of intersecting pores with in the crystal. The pore structure consists of two intersecting channel systems as shown in Figure 3.5 b : one straight and the other sinusoidal and the perpendicular to the former [48]. Many molecules are small enough to penetrate into this intracrystalline pore structure, where they may be crystallitically converted.

The properties of a zeolite depend on the structure of zeolite, the size of the free channels, the presence of faults and occluded material, and the ordering of T atoms (framework metal atoms). Therefore, structural information is important in understanding the adsorptive and catalytic properties of zeolites [52].

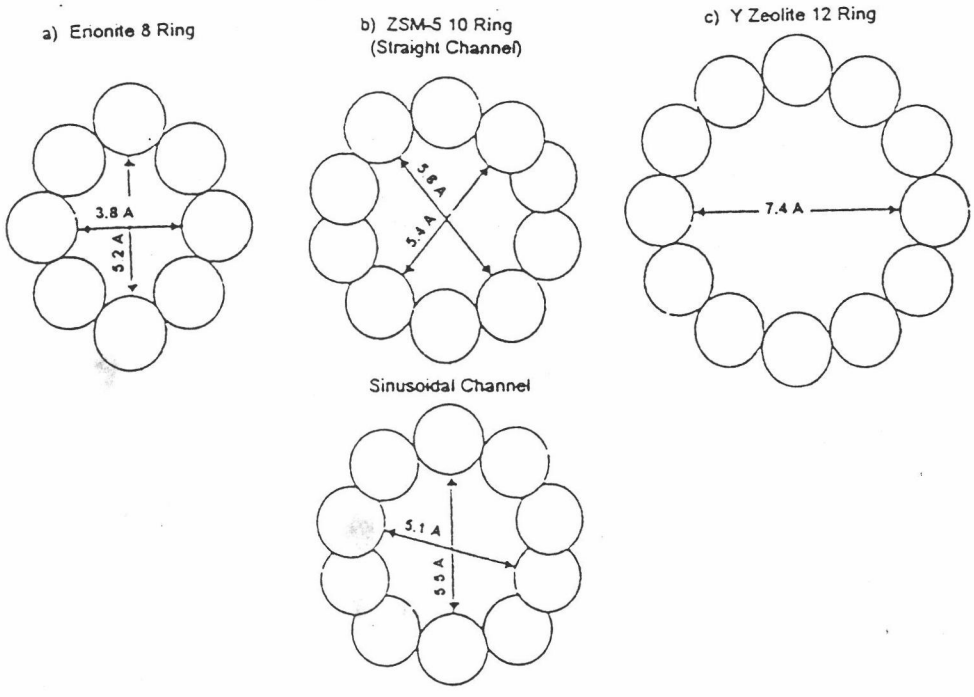


Figure 3.3 Typical zeolite pore geometries [48].

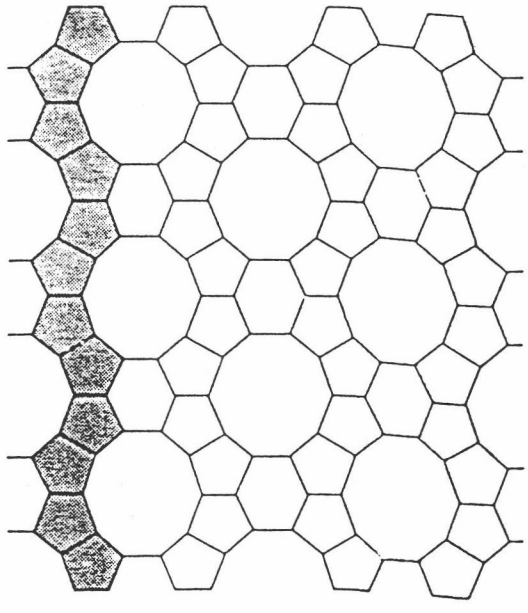

Figure 3.4 Schematic diagram of silicalite layers, formed by linking of the chains through sharing of oxygen in linked $SiO_4$ tetrahedra [51].

### 3.2.2 Non-aluminosilicate Molecular Sieves

The aluminosilicate zeolites offer the ion exchange properties, higher thermal stability, high acidity and shape-selective structural features desired by those working in the areas of adsorption and catalysis. However, modification and subsequent improvement of these properties have served as a driving force for changing the composition of these microporous materials [46].

Advances in the area of new molecular sieve materials have come in the preparation of zeolite-like structure containing framework components other than aluminum and silicon exclusively. There are now many non-aluminosilicate molecular sieves [52]. Referring to Figure 3.2, if tetrahedra containing aluminum and phosphorous, which is aluminophosphate or $AlPO_4$, are connected in a strict Al/P = 1, a neutral framework is obtained. Also, other elemental can be incorporated into $AlPO_4$ framework to make them changed, e.g., silicoaluminophosphates or SAPO's. Phosphate-based molecular sieves have extended the pore size range from 8A° to 13 A°. Figure 3.6 shows some typical framework projections containing various rings (pores) of different sizes. However, it should be noted that the data shown for cloverite and $AlPO_4$-8 are the maximum dimension as determined from the crystal structure. For $AlPO_4$-8 , the structure is faulted and the adsorption behavior that would be expected from the crystal structure cannot be obtained [52]. Also, adsorption data revealing the size of clovertite is not yet reported [52].

## 3.3 Acidity of Zeolite

Classical Brønsted and Lewis acid models of acidity have been used to classify the active sites on zeolites. Brønsted acidity is proton donor acidity; a trigonally coordinated alumina atom is an electron deficient and can accept an electron pair, therefore behaves as a Lewis acid [53,54].

In general, the increase in Si/Al ratio will increase acidic strength and thermal stability of zeolite [55]. Since the number of acidic OH groups depend on the number of aluminum in zeolite's framework, decrease in Al content is expected to reduce catalytic activity of zeolite.

Based on electrostatic consideration, the charge density at a cation site increase with increasing Si/Al ratio. It was conceived that this Phenomenon is related to the

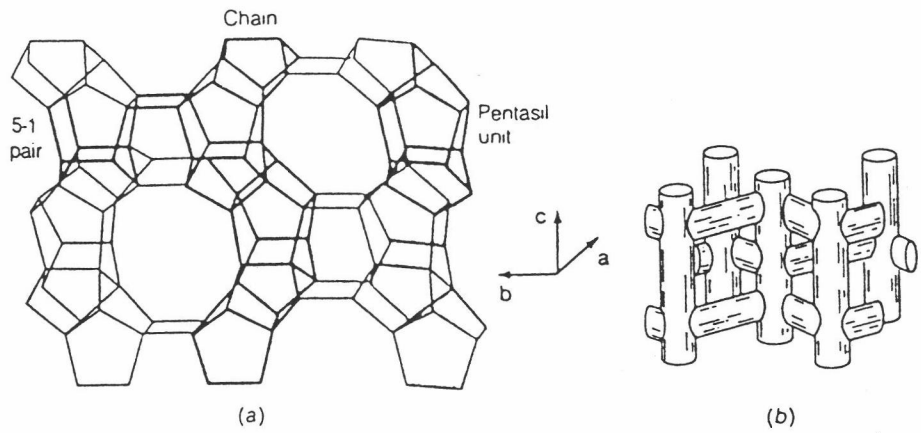


Figure 3.5 Three-dimensional structure of silicalite (ZSM-5) [51].

(a) Structure formed by stacking of sequences of layers.

(b) Channel network.

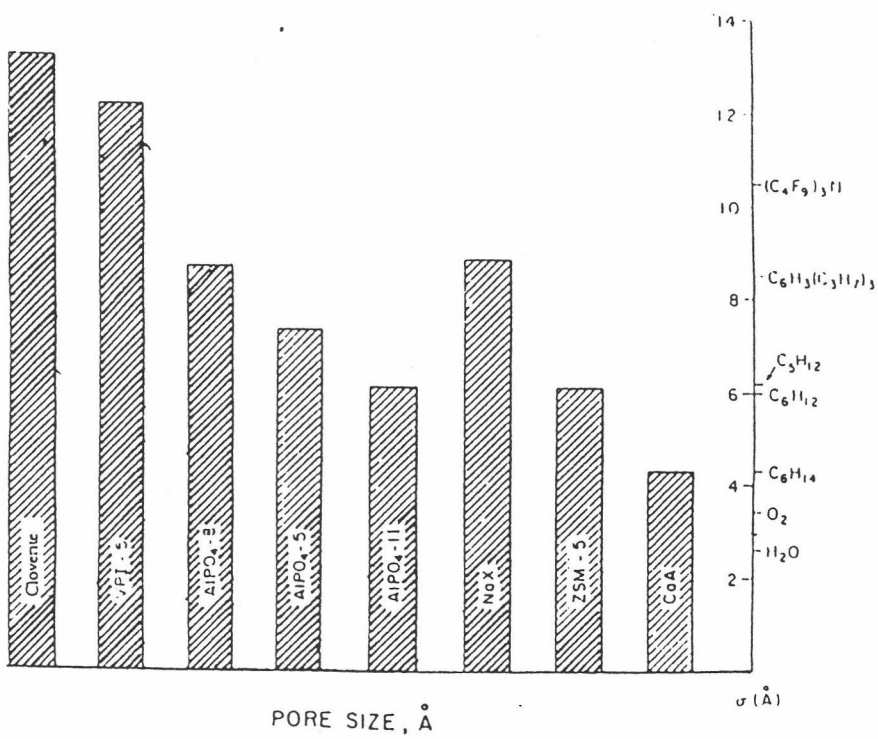


Figure 3.6 Typical zeolites pore sizes compared to the diameter of various molecules [52].

reduction of electrostatic interaction between framework sites, and possibly to the difference in the order of aluminum in zeolite crystal [54].

It has been reported the mean charge on the proton was shifted regularly towards higher values and the Al content decreased [53]. Simultaneously the total number of acidic hydroxyls, governed by the Al atoms, were decreased. This evidence emphasized that the entire acid strength distribution (weak, medium, strong) was shifted towards stronger values. That is, weaker acid sites become stronger with the decrease in Al content.

An improvement in thermal or hydrothermal stability has been ascribed to the lower density of hydroxyls groups which parallel to that of Al content [48]. A longer distance between hydroxyl groups decreases the probability of dehydroxylation that generates defects on structure of zeolites.

### 3.4 Generation of Acid Centers

Protonic acid centers of zeolite are generated in various ways. Figure 3.7 depicts the thermal decomposition of ammonium exchanged zeolites yielding the hydrogen form [46].

The BrØnsted acidity due to water ionization on polyvalent cations described below, is depicted in Figure 3.8 [48].

$$Mn^{+} + xH_2O \longrightarrow M(OH)_x^{(n-x)+} + xH^{+} \qquad (3.1)$$

The exchange of monovalent ions by polyvalent cation could improve the catalytic property. Those highly charged cations create very acidic centers by hydrolysis phenomenon.

BrØnsted acid site are also generated by the reduction of transition metal cations. The concentration of OH groups of zeolite containing transition metals was noted to increase by reduction with hydrogen at 250-450 °C and to increase by reduction with the rise of the reduction temperature [48].

$$Cu^{2+} + H_2 \longrightarrow Cu^{0} + 2H^{+} \qquad (3.2)$$

$$Ag^{+} + 1/2H_2 \longrightarrow Ag^{0} + H^{+} \qquad (3.3)$$

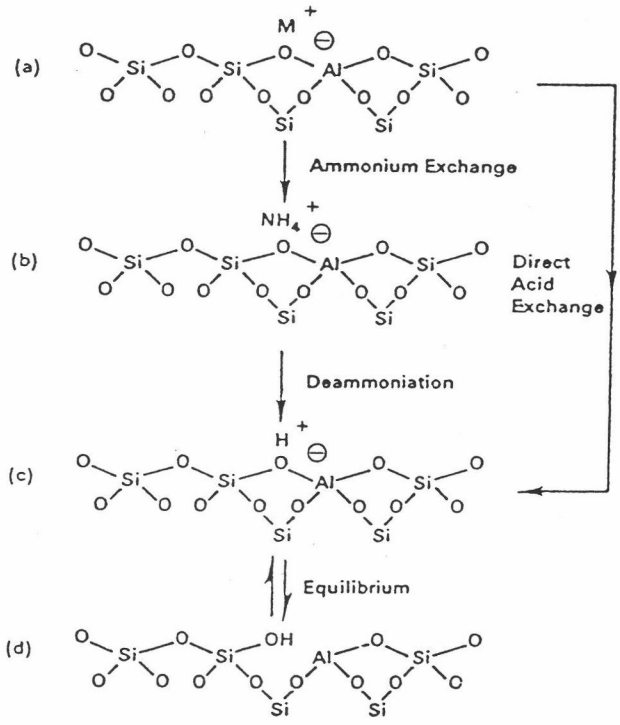


Figure 3.7 Diagram of the surface of zeolite framework [46].

(a) In the as-synthesized form $M^{+1}$ is either an organic cation or an alkalimetal cation.

(b) Ammonium in exchange produces the $NH_4^+$ exchanged form.

(c) Thermal treatment is used to remove ammonia, producing the $H^{+1}$ acid form.

(d) The acid form in (c) is in equilibrium with the form shown in (d), where there is a silanol group adjacent to a tricoordinate aluminum.

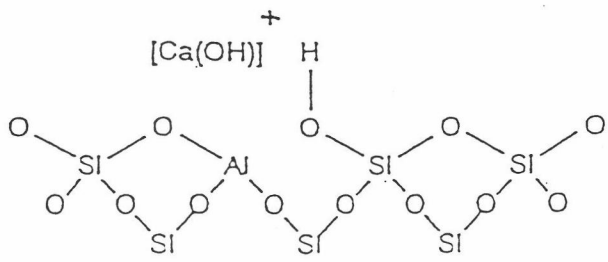


Figure3.8 Water molecules coordinated to polyvalent cation are dissociated by heat treatment yielding Bronsted acidity [48].

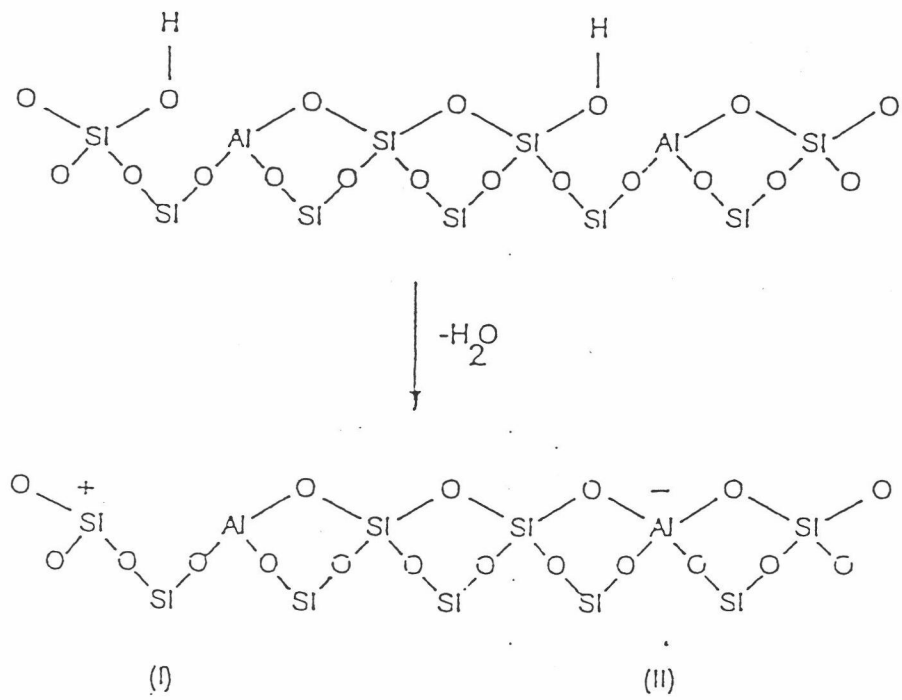


Figure 3.9 Lewis acid site developed by dehydroxylation of Bronsted acid site [48].

The formation of Lewis acidity from Brønsted sites is depicted in Figure 3.9 [48]. The dehydration reaction decreases the number of protons and increases that of Lewis sites.

Brønsted (OH) and Lewis (Al) sites can be present simultaneously in the structure of zeolite at high temperature. Dehydroxylation is thought to occur in ZSM-5 zeolite above 500 °C and calcination at 800 to 900 °C produces irreversible dehydroxylation which causes defection in crystal structure of zeolite.

Dealumination is believed to occur during dehydroxylation which may result from the steam generation with in the sample [48]. the dealumination indicated by an increase in surface concentration of aluminum on the crystal. The dealumination process is expressed in Figure 3.10 [48]. The extent of dealumination monotonously increases with the partial pressure of steam.

The enhancement of acid strength of OH groups is recently proposed to be partinent to their interaction with those aluminum species sites and are tentatively expressed in Figure 3.11 [48]. Partial dealumination might, therefore, yield a catalyst of higher activity while severe steaming reduces the catalytic activity.

### 3.5 Shape Selectivity

There are several types of shape and size selectivity in zeolites. Firstly, reactant or charge selectivity results from the limited diffusibility of some of reactants, which cannot effectively enter and diffuse inside crystal pore structures of the zeolites. A particularly good illustration of this behavior is given by Weisz and co-workers [56]. Zeolites A and X were ion exchanged with calcium salts to create acid sites within the zeolite. These acid sites are formed as the water of hydration around the calcium ions hydrolyzes. When these zeolites are contacted with primary and secondary alcohol dehydrate on CaX but only the primary one reacts on CaA. Since the secondary alcohol is too large to diffuse through the pores of CaA, it cannot reach the active sites within the CaA crystals. This kind of selectivity is called reactant shape selectivity and is illustrated in Figure 3.12 (a).

Product shape selectivity occurs when reaction products of different sizes are formed within the interior of the zeolite crystals and some of the products formed within the interior of the zeolite crystals and some of the products formed are too

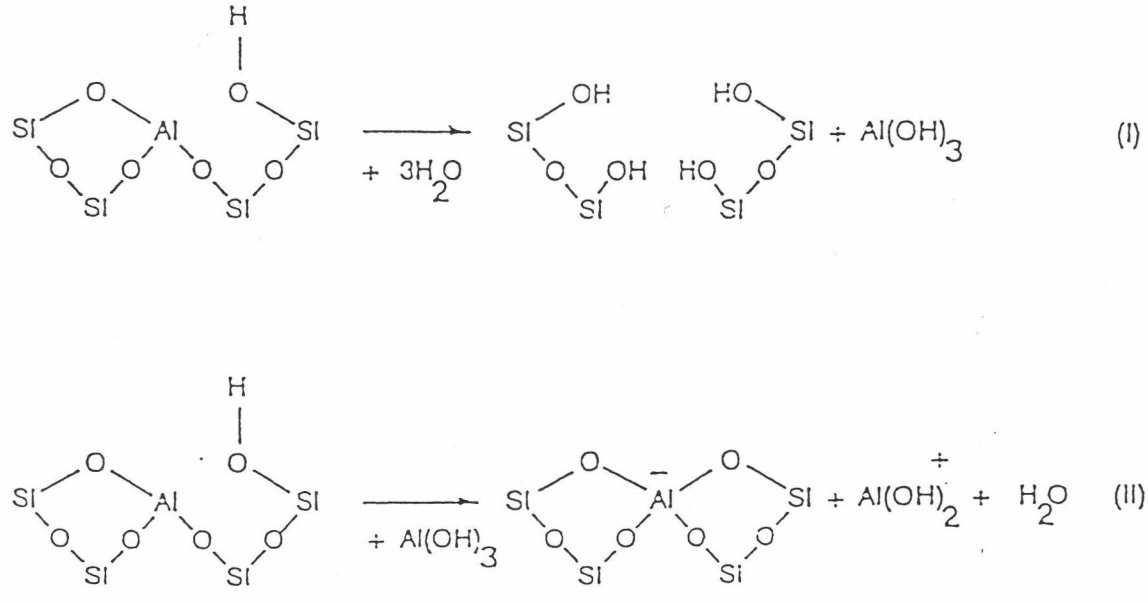


Figure 3.10 Steam dealumination process in zeolite [48].

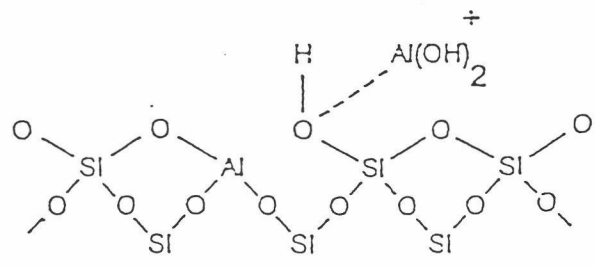


Figure 3.11 The enhancement of the acid strength of OH groups by their interaction with dislodged aluminum species [48].

bulkly to diffuse out [57]. The products which cannot escape from the cavities may undergo secondary reaction to smaller molecules or may deactivate the catalyst by blocking pores. A classic example of this type of selectivity is the monomolecular isomerization reactions of alkylaromatics as depicted in Figure 3.12 (b). The diffusion coefficient for para-xylene. Hence, essentially pure para-xylene is observed leaving the zeolite. Direct evidence for this type of shape selectivity has been reported by Anderson and Klinowski [58] for the catalytic conversion of methanol to hydrocarbons in ZSM-5. During the reaction, methanol is dehydrated to dimethyl ether (DME). The equilibrium mixture between methanol and DME reacts to form olefins, aliphatics and aromatics. By using in situ magic angle spinning NMR, 29 different organic species were identified in the adsorbed phase; however not all of these were observed with gas chromatography. For example, the tetramethylbenzenes that are formed in the pores of ZSM-5 do not diffuse out from the zeolites to be observed with gas chromatography.

Another type of shape selectivity is transition-state shape selectivity. For this type of selectivity, certain types of transition-state intermediates are too large to be accommodated within the pores/cavities of the zeolites. However, neither the reactants or the products are restricted from diffusing through the pores of zeolites. A good example of this type of selectivity is the transalkylation of dialkylbenzenes. In this reaction, an alkyl group is transferred from one molecule to another through a diphenylmethane transition state. For meta-xylene, this reaction will produce 1,3,5- as well as 1,2,4-trislkylbenzene. However, the transition state for the reaction that yields 1,3,5-trialkylbenzene is too large to be accommodated within the pore of mordenite. Consequently, only 1,2,4-trialkylbenzene is selectively formed inside the zeolite as illustrated in Figure 3.12 (c).

The critical diameter (as opposed to the length) of the molecules and the pore channel diameter of zeolites are important in predicting shape selective effects. However, molecules are deformable and can pass through opening which are smaller than their critical diameters. Hence, not only size but also the dynamics and structure of the molecules must be taken into account.

a) Reactant selectivity

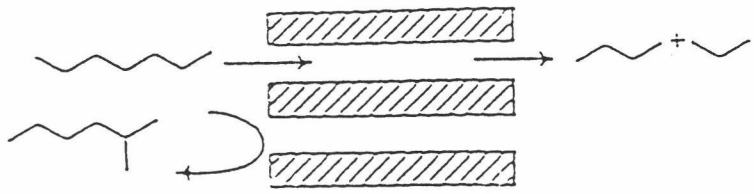

b) Product selectivity

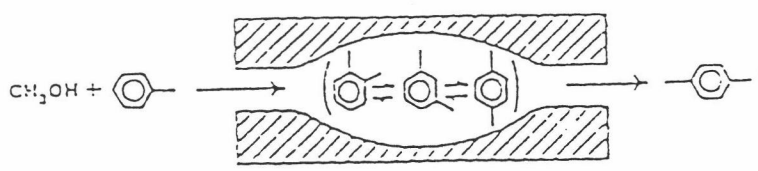

c) Transient state selectivity

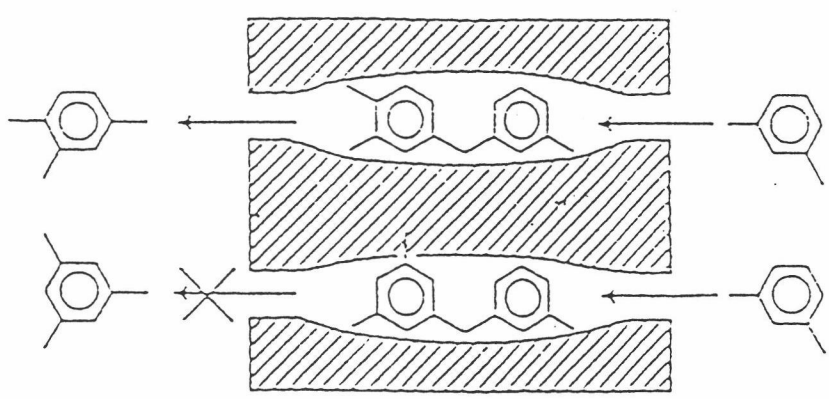

Figure 3.12 Schematic representation of the types of shape selectivity exhibited by zeolites [56].

Table 3.1 Kinetic diameters of various molecules based on the Leonard-Jones relationship [59].

| | Kinetic Diameter (Angstroms) |
|---|---|
| He | 2.6 |
| $H_2$ | 2.89 |
| $O_2$ | 3.46 |
| $N_2$ | 3.64 |
| NO | 3.17 |
| CO | 3.76 |
| $CO_2$ | 3.3 |
| $H_2O$ | 2.65 |
| $NH_3$ | 2.6 |
| $CH_4$ | 3.8 |
| $C_2H_2$ | 3.3 |
| $C_2H_4$ | 3.9 |
| $C_3H_8$ | 4.3 |
| n-$C_4H_{10}$ | 4.3 |
| Cyclopropane | 4.23 |
| i-$C_4H_{10}$ | 5.0 |
| $SF_6$ | 5.5 |
| Neopentane | 6.2 |
| $(C_4F_9)_3N$ | 10.2 |
| Benzene | 5.85 |
| Cyclohexane | 6.0 |

Table 3.1 [59] presents values of selected critical molecular diameters and table 3.2 [46] presents value of the effective pore size of various zeolites correlation between pore size of zeolites and kinetic diameter of some molecules are depicted in Figure 3.13 [60].

Table 3.2. Shape of the pore mouth opening of known zeolite structures. The dimensions are based on two parameters, the T atom forming the channel opening (8, 10, 12 rings) and the crystallographic free diameters of the channels. The channels are parallel to the crystallographic axis shown in brackets (e.g. <100>) [46].

| Structure | 8-Member ring | 10-Member ring | 12-Member ring |
|---|---|---|---|
| Biditaite | 3.2*4.9[001] | | |
| Brewsterite | 2.3*5.0[100] | | |
| | 2.7*4.1[001] | | |
| Cancrinite | | | 6.2[001] |
| Chabazite | 3.6*3.7[001] | | |
| Dachiardite | 3.6*4.8[001] | 3.7*6.7[010] | |
| TMA-E | 3.7*4.8[001] | | |
| Edingtonite | 3.5*3.9[110] | | |
| Epistilbite | 3.7*4.4[001] | 3.2*5.3[100] | |
| Erionite | 3.6*5.2[001] | | |
| Faujasite | | | 7.4<111> |
| Ferrierite | 3.4*4.8[010] | 4.3*5.5[001] | |
| Gismondine | 3.1*4.4[100] | | |
| | 2.8*4.9[010] | | |
| Gmelinite | 3.6*3.9[001] | | 7.0[001] |
| Heulandite | 4.0*5.5[100] | 4.4*7.2[001] | |
| | 4.1*4.7[001] | | |
| ZK-5 | 3.9<100> | | |
| Laumontite | | 4.0*5.6[100] | |
| Levyne | 3.3*5.3[001] | | |
| Type A | 4.1<100> | | |
| Type L | | | 7.1[001] |
| Mazzite | | | 7.4[001] |
| ZSM-11 | | 5.1*5.5[100] | |
| Merlinoite | 3.1*3.5[100] | | |
| | 3.5*3.5[010] | | |
| | 3.4*5.1[001] | | |
| | 3.3*3.3[001] | | |
| ZSM-5 | | 5.4*5.6[010] | |
| | | 5.1*5.5[100] | |
| Mordenite | 2.9*5.7[010] | | 6.7*7.0[001] |
| Natrolite | 2.6*3.9<101> | | |
| Offretite | 3.6*5.2[001] | | 6.4[001] |
| Paulingite | 3.9<100> | | |
| Phillipsite | 4.2*4.4[100] | | |
| | 2.8*4.8[010] | | |
| | 3.3[001] | | |